JOURNAL OF VIROLOGY, May 2001, p. 4080–4090 Vol. 75, No. 9
0022-538X/01/$04.00+0 DOI: 10.1128/JVI.75.9.4080–4090.2001

Adeno-Associated Virus Type 2-Mediated Gene Transfer: Altered Endocytic Processing Enhances Transduction Efficiency in Murine Fibroblasts

JONATHAN HANSEN,[1,2,3] KEYUN QING,[1,2,3] AND ARUN SRIVASTAVA[1,2,3,4]*

Department of Microbiology & Immunology,[1] Walther Oncology Center,[2] and Division of Hematology/Oncology,[4] Department of Medicine, Indiana University School of Medicine, and Walther Cancer Institute,[3] Indianapolis, Indiana 46202

Received 22 November 2000/Accepted 30 January 2001

Adeno-associated virus type 2 (AAV) is a single-stranded-DNA-containing, nonpathogenic human parvovirus that is currently in use as a vector for human gene therapy. However, the transduction efficiency of AAV vectors in different cell and tissue types varies widely. In addition to the lack of expression of the viral receptor and coreceptors and the rate-limiting viral second-strand DNA synthesis, which have been identified as obstacles to AAV-mediated transduction, we have recently demonstrated that impaired intracellular trafficking of AAV inhibits high-efficiency transduction of the murine fibroblast cell line, NIH 3T3 (J. Hansen, K. Qing, H. J. Kwon, C. Mah, and A. Srivastava, J. Virol. 74:992–996, 2000). In this report, we document that escape of AAV from the endocytic pathway in NIH 3T3 cells is not limited but processing within endosomes is impaired compared with that observed in the highly permissive human cell line 293. While virions were found in both early and late endosomes or lysosomes of infected 293 cells, they were localized predominantly to the early endosomes in NIH 3T3 cells. Moreover, treatment of cells with bafilomycin A1 (Baf), an inhibitor of the vacuolar H^+-ATPase and therefore of endosomal-lysosomal acidification, decreased the transduction of 293 cells with a concomitant decrease in nuclear trafficking of AAV but had no effect on NIH 3T3 cells. However, after exposure of NIH 3T3 cells to hydroxyurea (HU), a compound known to increase AAV-mediated transduction in general, virions were detected in late endosomes and lysosomes, and these cells became sensitive to Baf-mediated inhibition of transduction. Thus, HU treatment overcomes defective endocytic processing of AAV in murine fibroblasts. These studies provide insights into the underlying mechanisms of intracellular trafficking of AAV in different cell types, which has implications in the optimal use of AAV as vectors in human gene therapy.

Adeno-associated virus type 2 (AAV) is a nonpathogenic human parvovirus that contains a single-stranded DNA genome and belongs to the genus *Dependovirus*, so named because it requires coinfection with a helper virus for efficient viral replication (8, 47). Both herpesvirus and adenovirus can provide the helper functions necessary for AAV to undergo a productive, lytic infection in which progeny virions are produced (7). In the absence of a helper virus, the wild-type AAV establishes a latent infection by integrating site specifically into human chromosome 19 (22, 23, 44). Although first isolated from rhesus monkey kidney cell cultures (3), evidence is accumulating that AAV can infect a wide variety of cells from various species, including humans and mice. These properties have been instrumental in the development of AAV as a vector for human gene therapy. Indeed, human clinical trials using recombinant AAV vectors in the treatment of cystic fibrosis and hemophilia B are under way (13, 21).

Although AAV infects most cell types examined thus far, a growing number of nonpermissive cell types have been identified (5, 35, 39). Furthermore, the transduction efficiency of "permissive" cells varies widely. By investigating basic aspects of AAV infection, we and others have begun to identify the obstacles to high-efficiency AAV-mediated transduction. For example, to be transduced, cells must express the proper combination of receptors and coreceptors on their surface. Heparan sulfate proteoglycan and human fibroblast growth factor receptor 1 have been identified as the viral receptor and coreceptor, respectively (39, 49). In addition, others have shown that $\alpha_V\beta_5$ integrin is a coreceptor for AAV and plays a key role during virus internalization (48). After binding, the virus enters the cell via clathrin-coated pits (9), traffics to the nucleus, uncoats, and must undergo a round of second-strand viral DNA synthesis to yield a transcriptionally active double-stranded DNA intermediate. Second-strand viral DNA synthesis is the rate-limiting step in AAV-mediated transduction (11, 12). We have identified a cellular protein, the single-stranded D-sequence binding protein (ssD-BP), which binds the D-sequence near the 3′ end of the viral genome and, when phosphorylated at tyrosine residues, inhibits the viral second-strand DNA synthesis (38, 40). Moreover, we have shown that human epidermal growth factor receptor protein tyrosine kinase activity phosphorylates the ssD-BP and therefore modulates the rate of the viral second-strand DNA synthesis (26).

Hydroxyurea (HU) treatment of cells has been postulated to increase the rate of AAV second-strand DNA synthesis by inducing a cellular microenvironment that results in dephos-

* Corresponding author. Mailing address: Department of Microbiology & Immunology, Indiana University School of Medicine, 635 Barnhill Dr., Medical Science Building Room 257, Indianapolis, IN 46202-5120. Phone: (317) 274-2194. Fax: (317) 274-4090. E-mail: asrivast@iupui.edu.

phorylation of the ssD-BP (40). In addition, others have proposed that HU increases AAV-mediated transduction by causing S-phase arrest with a concomitant increase in the DNA repair synthesis that normally occurs during DNA replication (42). The induction of DNA repair synthesis by genotoxic agents such as γ and UV irradiation increases transduction efficiency, indicating that the DNA repair machinery may be responsible for synthesizing the second strand of viral DNA since AAV lacks its own DNA polymerase (1, 2). Since HU arrests the cell cycle by inhibiting ribonucleotide reductase, resulting in depletion of the pool of deoxyribonucleotides required for DNA synthesis, one might expect that viral second-strand DNA synthesis would be impaired as well; therefore, the HU-induced increase in AAV-mediated transduction might be due to additional effects on the viral life cycle besides second-strand synthesis.

Despite intensive efforts to understand events surrounding the early steps of AAV infection, relatively little is known about how the virus traffics to the nucleus. Previously, we have demonstrated that impaired intracellular trafficking into the nucleus limits high-efficiency AAV-mediated transduction of murine fibroblasts (18). More recently, others have shown that passage through an acidic subcellular compartment is necessary for efficient viral transduction and that AAV utilizes microtubules, microfilaments, and a Rac1/phosphatidylinositol 3-kinase (PI3-kinase)-dependent mechanism to traffic to the nucleus (6, 45). Moreover, ubiquitination of viral capsids has been postulated as a mechanism whereby certain cell types can degrade the entering virions prior to nuclear translocation (10). These observations notwithstanding, no direct evidence of differential viral trafficking through endocytic organelles of permissive and less permissive cell types exists. We hypothesized that in less permissive cell types, AAV fails to enter the acidic late endosomes, rendering it deficient in its ability to continue to traffic into the nucleus and mediate transduction. In this report, we provide evidence that in permissive cells, AAV traffics through both early and late endosomes. However, in less permissive cell types, AAV fails to enter the late endosomes, which accounts, in part, for the decreased transduction efficiency of this cell type. Moreover, HU treatment of the less permissive cells prior to infection by AAV causes the virions to be processed through late endosomes, resulting in increased transduction efficiency. This effect is seen as early as 2 h after the addition of HU. These studies have implications for the optimal use of AAV vectors in the high-efficiency transduction of less permissive cell types.

MATERIALS AND METHODS

Cells, plasmids, and viruses. The adenovirus-transformed human embryonic kidney cell line 293 and the murine fibroblast cell line NIH 3T3 were obtained from the American Type Culture Collection (Manassas, Va.). Monolayer cultures of 293 and NIH 3T3 cells were maintained in Iscove's modified Dulbecco's medium (IMDM) supplemented with 10% newborn calf serum and antibiotics. Recombinant AAV plasmids CMVp-*lacZ*, containing the cytomegalovirus immediate-early promoter-driven β-galactosidase (*lacZ*) gene, and CMVp-luc, containing the CMVp-driven firefly luciferase gene, have been described elsewhere (27, 33, 34). Recombinant AAV vector (vCMVp-*lacZ* and vCMVp-luc) stocks were generated and purified by CsCl equilibrium density gradient centrifugation as previously described (24, 29, 33–36). Physical particle titers of recombinant vector stocks were determined by quantitative DNA slot blot analysis, as previously described (24, 25, 51). The contaminating wild-type AAV-like particle titers were approximately 0.01%.

Subcellular fractionation and detection of viral DNA. Approximately 8×10^6 cells were seeded in 10-cm tissue culture dishes and allowed to adhere for 18 h. The cells were then either mock treated or treated with 10 mM HU for 18 h, washed once with IMDM, and either mock infected or infected with 3,000 particles of vCMVp-*lacZ* per cell for 1 h at 37°C in IMDM. The cells were washed once with phosphate-buffered saline (PBS), trypsinized for 10 min at 37°C, and then washed twice with PBS to remove virions adsorbed to the plasma membrane. The remainder of the procedure was carried out at 4°C by previously described methods (15, 19). Briefly, after the cells were washed once in homogenization buffer (0.25 M sucrose, 10 mM triethanolamine [pH 7.6], 1 mM EDTA, 1 mM phenylmethylsulfonyl fluoride, 100 μg of aprotinin per ml), they were homogenized in a tight-fitting Duall tissue grinder (Fisher Scientific, Pittsburgh, Pa.) until about 60% cell lysis was achieved (about 15 strokes) as monitored by trypan blue uptake. The nuclei and intact cells were removed by centrifugation at $1,000 \times g$ for 5 min, and the postnuclear supernatant (PNS) was diluted to a final volume of 10 ml with homogenization buffer and then layered onto a 2-ml 1.5 M sucrose cushion. Samples were centrifuged at $200,000 \times g$ in an SW41 Ti ultracentrifuge rotor for 15 h, and ~350-μl fractions were subsequently collected from the bottom of the tube. In some experiments, fractions at the top of the sucrose cushion, which contained the endocytic organelles, were pooled and diluted 1:4 in homogenization buffer and organelles were concentrated by ultracentrifugation at $135,000 \times g$ for 1 h. The organelles were then resuspended in 0.6 ml of homogenization buffer layered on a 3.4-ml Percoll solution (8% Percoll, 0.25 M sucrose) and separated by density gradient ultracentrifugation in a TLA-100.3 rotor at $35,000 \times g$ for 1 h. Fractions (0.5 ml each) were collected from the bottom of the tube, diluted 1:3 with dilution buffer (20 mM HEPES [pH 7.4], 1 mM PMSF, 100 μg of aprotinin per ml), after which organelles in each fraction were concentrated as described above and resuspended in 60 μl of dilution buffer. Fractions from either the sucrose cushion or the Percoll density gradient were then assayed for viral DNA by slot blot analysis as described previously (25), with the following modification. After the addition of NaOH, the samples were extracted once with phenol and once with chloroform prior to loading. The relative amount of viral DNA was estimated by densitometric scanning of autoradiograms with an Alphaimager digital imaging system (Alpha Innotech Corp., San Leandro, Calif.). In some experiments, nuclear and PNS fractions from infected cells were isolated and viral DNA was detected by Southern analysis as described previously (18).

Isolation of cytoplasmic virions. Approximately 8×10^6 293 or NIH 3T3 cells were infected for 1 h at 37°C with 20,000 particles of vCMVp-luc per cell, trypsinized, washed twice with PBS, and homogenized as described above. Following centrifugation and fractionation of the PNS on a sucrose cushion as described above, the first four fractions were pooled and diluted in PBS, and virions in these fractions were concentrated using Centricon-30 centrifugal filter devices (Amicon, Beverly, Mass.) as specified by the manufacturer. The physical titers of virus were determined by quantitative slot blot analysis as above, and an equivalent number of particles isolated from each cell type was assayed for transduction efficiency as described below.

Recombinant AAV transduction assays. Approximately 10^5 cells per well were seeded into 12-well tissue culture plates. At 18 h later, the cells were washed once with PBS and then either mock treated or exposed to 20 nM bafilomycin A1 (Baf) for 1 h, 750 μM tyrphostin 1 for 2 h, or 10 mM HU for various times at 37°C. All inhibitors were purchased from Sigma (St. Louis, Mo.), and stock solutions were prepared in dimethyl sulfoxide, except HU, which was dissolved in PBS. HU was replaced every 8 h during extended treatments. After the cells were rinsed once with IMDM, they were incubated for 2 h at 37°C with IMDM either alone or containing 5,000 particles of vCMVp-*lacZ* per cell. A 2-ml volume of IMDM containing 10% newborn calf serum was then added, and 48 h later the β-galactosidase activity was measured by the Galacto-Light Plus chemiluminescent reporter assay (Tropix, Inc., Bedford, Mass.) as specified by the manufacturer. Data were expressed as relative light units (RLU) per microgram of total protein as determined by a protein assay (Bio-Rad, Hercules, Calif.). In some experiments, prior to infection, vCMVp-luc was preincubated for 30 min at 37°C in either PBS (pH 7.0) or an acidic buffer (100 mM sodium citrate [pH 3.0], 150 mM NaCl) and subsequently diluted 1:100 in IMDM. When vCMVp-luc was used, luciferase activity was measured 48 h postinfection by using the luciferase assay system with reporter lysis buffer (Promega, Madison, Wis.) as specified by the manufacturer. Data were also expressed as RLU per microgram of total protein.

Analysis of markers for endocytic organelles. To label the early endosomes, cells were pulsed with 30 μg of biotinylated human holotransferrin (Sigma) per ml for 10 min at 37°C in IMDM. After the cells were harvested and endocytic organelles were isolated as outlined above, proteins in 20 μl of each fraction were separated by sodium dodecyl sulfate-polyacrylamide gel electrophoresis through

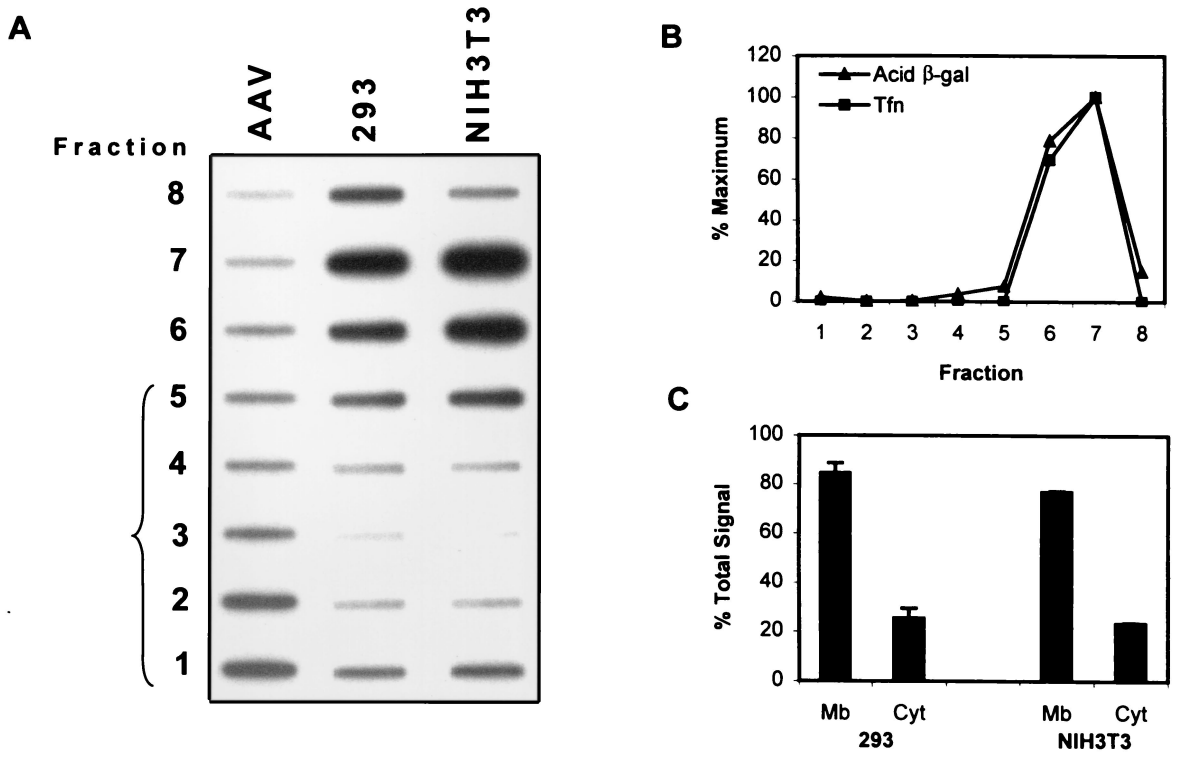

FIG. 1. (A) Slot blot analysis of viral DNA in membranes and cytoplasm of cells. Equivalent numbers of 293 or NIH 3T3 cells were infected for 1 h with the recombinant vCMVp-*lacZ* (3,000 particles/cell) and homogenized, and the membranes were separated on a sucrose cushion by ultracentrifugation as described in Materials and Methods. Fractions were collected from the bottom of the tube, and viral DNA was quantified by slot blot analysis using the ^{32}P-labeled *lacZ* DNA probe as described previously (25). The bracket identifies the fractions containing the sucrose cushion. As a control, purified AAV virions were also loaded onto the sucrose cushion. (B) Analysis of endocytic markers. Cells were pulsed for 10 min with biotinylated holotransferrin prior to separation of homogenate on the sucrose cushion. Each fraction was then analyzed by Western blotting for the presence of biotinylated transferrin (Tfn), an early endosome marker, and by an enzymatic assay for acid β-galactosidase (Acid β-gal) activity, a lysosomal marker. Results are reported as percentages of the maximum signal intensity based on densitometric scanning of the autoradiogram or percentages of maximum enzymatic activity. (C) Subcellular distribution of AAV. Autoradiograms from three separate experiments similar to that in panel A were densitometrically scanned, and the signal intensities in each fraction were quantified. The combined values from fractions 1 to 4 and 5 to 8 were averaged and represent the amounts of AAV DNA in the cytoplasm (Cyt) and membranes (Mb), respectively.

a 12% polyacrylamide gel and transferred to an Immobilon-P membrane (Millipore Corp., Bedford, Mass.) as described elsewhere (43). The membrane was subsequently blocked in TBST-MLK (137 mM NaCl, 20 mM Tris [pH 7.6], 0.1% Tween 20, 5% nonfat dry milk) for 1 h at 25°C, washed three times in TBST, and incubated with a 1:1,000 dilution of horseradish peroxidase-conjugated anti-biotin antibody (New England Biolabs, Beverly, Mass.) in TBST-MLK for 1 h at 25°C. After three washes in TBST, the membrane was incubated with the ECL-Plus chemiluminescent substrate (Amersham, Little Chalfont, England) for 3 min and exposed to X-ray film. The relative amounts of biotinylated transferrin in each fraction were determined by densitometric scanning of the film as above. Acid β-galactosidase activity, a marker for lysosomes, was measured as described previously (46). Briefly, a 10-μl aliquot of each fraction from above was added to 100 μl of reaction buffer (200 mM sodium citrate [pH 4.0], 0.1% Triton X-100) containing 0.6 mg of 4-methylumbelliferyl-β-D-galactoside (Sigma) per ml and incubated at 37°C for 45 min. A 1-ml volume of stop buffer (133 mM glycine, 67 mM NaCl, 83 mM sodium carbonate [pH 10.6]) was added to each sample, and fluorescence was measured in an A-4 fluorometer (Optical Technology Devices, Inc., Elmsford, N.Y.) with an excitation wavelength of 370 nm and emission at 460 to 500 nm.

RESULTS

Escape from the endocytic pathway is not a rate-limiting step for AAV-mediated transduction of NIH 3T3 cells. We have recently demonstrated that impaired intracellular trafficking of AAV into the nucleus limits high-efficiency transduction of the murine fibroblast cell line NIH 3T3 (18). To more precisely determine the mechanisms responsible for decreased transduction of this cell type, we undertook a systematic examination of the steps in viral trafficking and processing and compared the results with those obtained with the highly permissive human embryonic kidney cell line 293. Since it has been previously established that AAV enters the endocytic pathway of the cell via clathrin-coated pits (9) and since we have demonstrated efficient entry of AAV into NIH 3T3 cells (18), we hypothesized that the virions failed to escape from the endocytic vesicles into the cytoplasm of NIH 3T3 cells and were therefore unable to subsequently traffic into the nucleus. To test this hypothesis, we infected 293 and NIH 3T3 cells with vCMVp-*lacZ* for 1 h. Following homogenization and removal of the nuclei by centrifugation, the PNS was layered onto a sucrose cushion and the cytoplasmic virions were separated from those in cellular organelles by ultracentrifugation. Fractions were collected from the bottom of the tube, and the amount of viral DNA in each fraction was detected by slot blot analysis. As shown in Fig. 1A, purified virions entered the

sucrose cushion, concentrating toward the bottom of the tube. In contrast, the virions isolated from the homogenate of infected 293 cells remained predominantly at the top of the sucrose cushion, presumably still within endocytic vesicles, although a small proportion of the total signal was detected at the bottom of the tube, indicating that some of the virions were indeed in the cytoplasm as expected. Similar results were obtained with infected NIH 3T3 cells (Fig. 1A). Transferrin and acid β-galactosidase activity, markers for light (early) endosomes and dense lysosomes, respectively, were concentrated in fractions at the top of the sucrose cushion, indicating that both light and dense endocytic organelles failed to penetrate the sucrose cushion under these conditions (Fig. 1B). Similar distributions of endocytic markers were observed for both 293 and NIH 3T3 cells. Autoradiograms similar to that in Fig. 1A from three independent experiments were scanned, and the signals were quantitated by densitometry. The signals in fractions 1 to 4 and 5 to 8 were summed and plotted as cytoplasmic and membrane fractions, respectively. The results are shown in Fig. 1C. Thus, 1 h postinfection, roughly 20% of the virions were found in the cytoplasm and 80% were found in the endocytic organelles. Because the results in the less permissive NIH 3T3 cells were similar to those in the more permissive 293 cells, we concluded that endosomal escape of AAV into the cytoplasm was not impaired in NIH 3T3 cells.

AAV fails to traffic through dense endocytic organelles in NIH 3T3 cells. Since similar proportions of AAV appeared to escape the endocytic pathway in both cell types and since 80% of the virions were associated with membranous organelles, we next hypothesized that differential processing of AAV within the vesicles of the endocytic pathway of NIH 3T3 cells was responsible for the lack of trafficking to the nucleus. Since it has been previously demonstrated in HeLa cells that passage through an acidic compartment is necessary for efficient AAV-mediated transduction (6), we hypothesized that failure of the virus to be processed in the acidic vesicles of NIH 3T3 cells may account for the decreased transduction efficiency. Since the endocytic pathway is composed of a series of organelles that become progressively more acidic and more dense, we reasoned that separation of the vesicles on a density gradient would directly demonstrate whether the virions entered the more dense, acidic vesicles in NIH 3T3 cells. To test this hypothesis, we infected equivalent numbers of cells with vCMVp-*lacZ* for 1 h at 37°C, isolated the membranes, separated the endocytic organelles on a Percoll density gradient, and subsequently detected viral DNA in each fraction of the gradient by slot blot hybridization to a ^{32}P-labeled *lacZ* probe, as described in Materials and Methods. These results are shown in Fig. 2A. It is clear that in the more permissive 293 cells, the AAV DNA was detected in both the lower and upper fractions, containing the dense and light endocytic organelles, respectively, whereas in the less permissive NIH 3T3 cells, viral DNA was detected only in the upper fractions. To ensure that the endocytic organelles were indeed separated by density under these conditions, we assayed each fraction for acid β-galactosidase activity and the presence of transferrin, markers for dense and light endocytic vesicles, respectively. As expected, most of the acid β-galactosidase activity was found in the fractions from the bottom of the gradient and transferrin was localized to the fractions from the top of the gradient, indicating that these conditions were appropriate for separating endocytic organelles according to density (Fig. 2B). The distribution of markers was similar for both cell types tested. Figure 2C is a plot of the average AAV signal intensities from each fraction in two separate experiments, as determined by densitometric scanning. These results provide evidence that virions are processed differently within the endocytic compartments of each cell type and that AAV passes through dense vesicles in 293 cells but not in NIH 3T3 cells.

Inhibiting the acidification of endocytic vesicles in NIH 3T3 cells does not affect AAV-mediated transduction efficiency. Although AAV localized differentially within the endocytic compartments of the permissive and less permissive cells, the role of endosomal acidification in the context of AAV-mediated transduction of the two cell types remained unknown. As early endosomes progress through the endocytic pathway, they become more dense and there is a concomitant decrease in luminal pH. Since AAV was found in the denser organelles of 293 but not NIH 3T3 cells, we hypothesized that endosomal acidification plays an essential role in the efficient transduction of 293 but not NIH 3T3 cells. To test this hypothesis, we pretreated 293 and NIH 3T3 cells for 2 h with 750 μM tyrphostin 1, a compound known to inhibit phosphorylation of the ssD-BP and permit unimpeded second-strand viral DNA synthesis (26). We also either mock treated or treated the cells for 1 h with 20 nM Baf, a specific and potent inhibitor of the vacuolar H^+-ATPase responsible for acidifying endocytic organelles. With the drugs still present, we infected the cells with 5,000 particles of vCMVp-*lacZ* per cell and assayed for β-galactosidase activity 48 h later. These results are shown in Fig. 3A. While the overall transduction of 293 cells was higher than that of NIH 3T3 cells, it is clear that Baf significantly inhibited the transduction of 293 cells but had little effect on the transduction of NIH 3T3 cells. That Baf inhibited the transduction of 293 cells is consistent with previously published data on the effect of Baf in AAV-mediated transduction of HeLa cells (6). However, the lack of Baf-mediated inhibition of transduction in NIH 3T3 cells indicated that the virions did not pass through acidified vesicles in this cell type. Moreover, the use of other agents, such as ammonium chloride and chloroquine, which prevent the acidification of organelles by a different mechanism yielded transduction data similar to those observed with Baf pretreatment (data not shown). These results were as expected since in 293 cells, the virions entered the dense acidic vesicles, which would be more sensitive to the pH-altering effects of the drugs than would the early endosomes involved in AAV trafficking in NIH 3T3 cells (Fig. 2). To verify that the Baf-mediated inhibition of transduction of 293 cells was due to decreased overall trafficking of AAV into the nucleus, we isolated nuclear fractions and PNS from 293 cells that had been either mock treated or treated with Baf and subsequently infected with vCMVp-*lacZ*. The low-M_r DNA from each fraction was analyzed by Southern blotting with a ^{32}P-labeled *lacZ* probe. As shown in Fig. 3B, most of the single-stranded viral DNA was detected in the nuclei of mock-treated 293 cells, which is consistent with previously published data (18). However, in Baf-treated cells, the viral DNA remained predominantly in the PNS and less was found in the nucleus. Taken together, these data demonstrate that endosomal acidification is necessary for the efficient trafficking of AAV into the nuclei

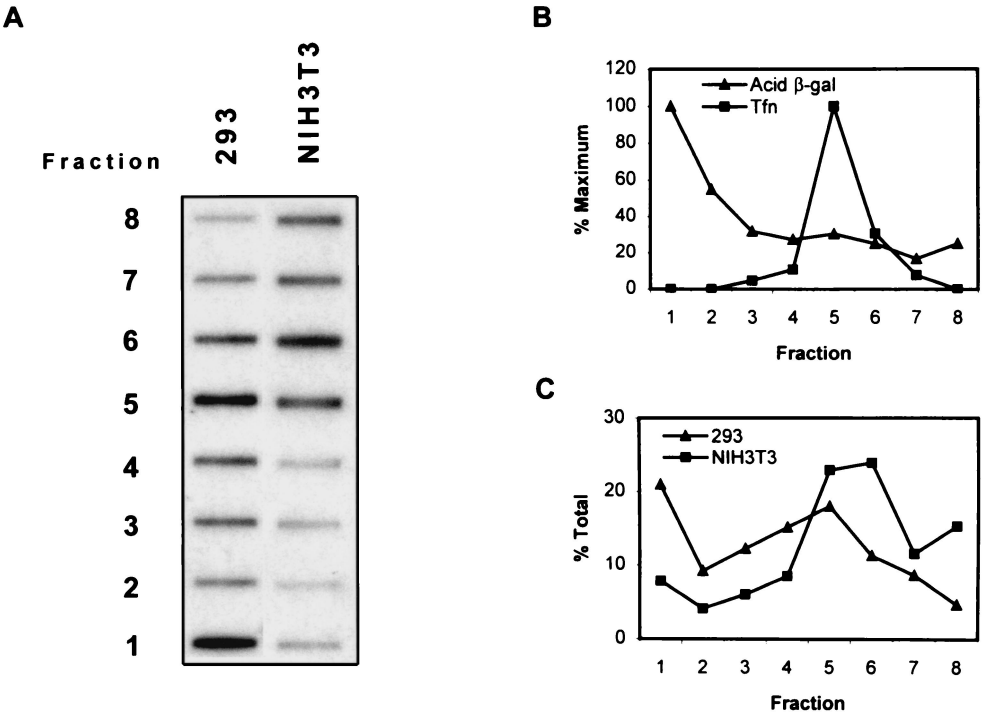

FIG. 2. (A) Slot blot analysis of viral DNA in endocytic organelles from cells. Equivalent numbers of 293 or NIH 3T3 cells were infected for 1 h with vCMVp-*lacZ* (3,000 particles/cell) and homogenized, and the membranes were separated on a Percoll density gradient as described in Materials and Methods. Fractions collected from the bottom of the tube were then analyzed for the presence of viral DNA by slot blot hybridization as described in the legend to Fig. 1. (B) Detection of endosomal and lysosomal markers. For each fraction, markers for early endosomes (Tfn) and lysosomes (Acid β-gal) were assayed as described in the legend to Fig. 1, and the results are shown as percentages of the maximum signal. (C) Distribution of AAV within endocytic vesicles. Autoradiograms similar to that in panel A from two separate experiments were densitometrically scanned, and the viral DNA in each faction was quantified, averaged, and plotted as a percentage of the total signal.

of 293 cells. In addition, since viral DNA was not detected in dense, acidic endosomes of NIH 3T3 cells, the transduction efficiency was about 100-fold lower and not sensitive to Baf treatment. This may explain, in part, the decreased nuclear trafficking of AAV in NIH 3T3 cells noted previously (18).

The AAV capsid structure may be modified in infected 293 but not in NIH 3T3 cells which impairs its infectivity in secondary infections. Ligands that undergo receptor-mediated endocytosis are subsequently processed through the endocytic pathway. In some instances, changes in the luminal pH of the vesicle are sufficient to cause alterations in ligand-receptor interactions (16). Moreover, in the case of internalized exogenous antigens, passage of the antigen through various endocytic vesicles in antigen-presenting cells exposes it to conditions necessary for processing and presentation to immune cells such as low pH, protease activity, and reducing environments (14, 20, 41). Because many of these processes are dependent on enzymes that function only at an acidic pH and because we demonstrated a low-pH requirement for efficient AAV-mediated transduction of cells, we postulated that the virion may be modified as it passes through the acidic vesicles of the endocytic pathway prior to its escape into the cytoplasm. To monitor changes in the viral capsid, we isolated virions from the cytoplasm of 293 or NIH 3T3 cells 1 h following infection with 20,000 particles per cell of vCMVp-luc as described in Materials and Methods. Following slot blot analysis to determine the physical titer of the isolated virions, we infected 293 cells with equivalent numbers of vCMVp-luc isolated from the cytoplasm of each cell type and assayed for luciferase activity 48 h postinfection. These results are shown in Fig. 4A. The virions isolated from the cytoplasm of 293 cells had about 33% of the transducing ability of the virions isolated from the cytoplasm of NIH 3T3 cells. While this experiment was an indirect measurement of capsid modification and did not provide information regarding the nature of the alteration, it did indicate that the virions isolated from the cytoplasm of 293 cells had been altered in a way that decreased their infectivity when added to the extracellular medium. Since AAV passes through acidic vesicles in 293 cells but not NIH 3T3 cells, we reasoned that exposure of the virion to acidic pH alone might be sufficient to account for the decrease in transducing ability of the virions isolated from the cytoplasm of 293 cells. Therefore, we preincubated purified vCMVp-luc in buffers of either pH 3.0 or 7.0 for 30 min at 37°C, diluted the solutions in IMDM to neutralize the pH, and then infected equivalent numbers of 293 cells. At 48 h postinfection, we assayed for luciferase activity. As shown in Fig. 4B, preincubation of the virions at pH 3.0 did not decrease their ability to transduce 293 cells compared with the ability of control virions incubated at pH 7.0. These results are consistent with previously published data that AAV retains its biological activity even in very acidic environments (4). However, we concluded that exposure to acidic conditions alone was insufficient to cause the modification of the virion that resulted in the decreased transducing ability.

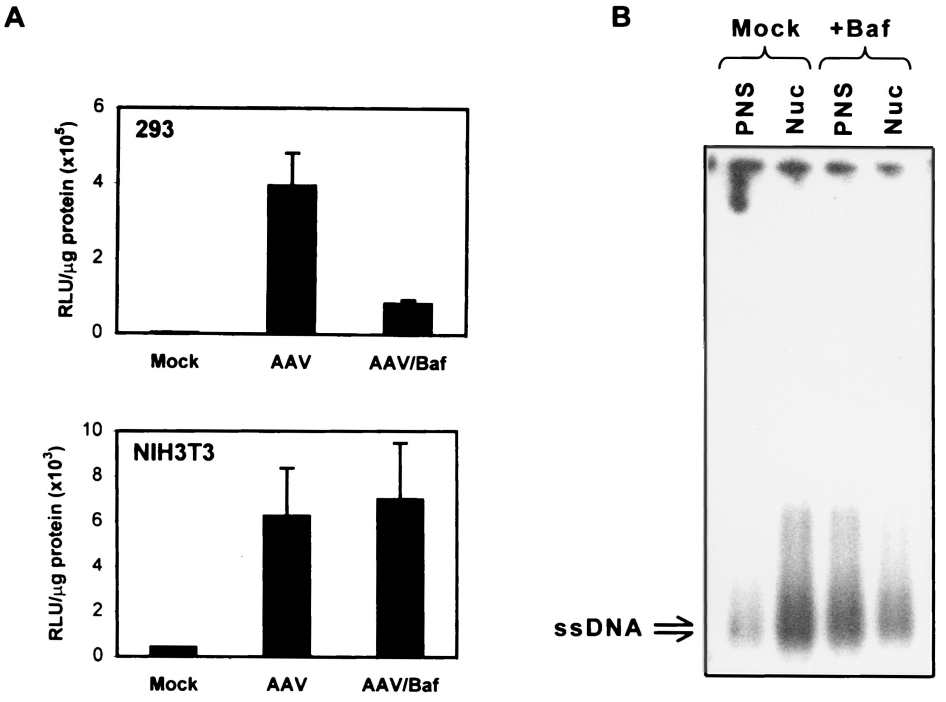

FIG. 3. (A) Effect of Baf on AAV-mediated transduction of 293 and NIH 3T3 cells. All cells were pretreated for 2 h with 750 μM tyrphostin 1 and incubated for 1 h with or without 20 nM Baf. The cells were then either mock infected or infected with vCMVp-*lacZ* (5,000 particles/cell) for 2 h, and transgene expression was measured 48 h later as described in Materials and Methods. Results are expressed in RLU per microgram of total protein. (B) Southern blot analysis of the subcellular distribution of viral DNA in Baf-treated cells. 293 cells were either mock treated or treated for 1 h with 20 nM Baf and subsequently infected with 5,000 particles of vCMVp-*lacZ* per cell for 2 h. The cells were trypsinized and washed, after which nuclear (Nuc) and PNS fractions were isolated as described previously (18). Low-M_r DNA was isolated from each fraction, and analyzed by Southern blotting using a ^{32}P-labeled *lacZ* probe. ssDNA denotes the viral single-stranded DNA genomes.

HU treatment alters endocytic trafficking of AAV in NIH 3T3 cells. It has become increasingly clear that AAV-mediated transduction of various cell types is impaired by a combination of factors. For instance, the lack of expression of viral receptors or coreceptors, the presence of tyrosine-phosphorylated ssD-BP with the accompanying inhibition of the viral second-strand DNA synthesis, and altered endocytic processing contribute to the decreased transduction of less permissive cell types. By identifying obstacles to AAV-mediated transduction, one could envisage means of overcoming these barriers. For example, it has been previously shown that HU treatment increases the transduction of many cell types, presumably by inducing the DNA repair synthesis machinery which may be crucial for viral second-strand DNA synthesis (42). Because HU depletes the intracellular stores of deoxyribonucleotides necessary for DNA synthesis by inhibiting ribonucleotide reductase, we reasoned that HU treatment of cells may actually limit viral second-strand DNA synthesis and that the increase in transduction efficiency observed previously might be due to additional effects such as increased nuclear trafficking of AAV. Indeed, we have recently observed in NIH 3T3 cells and primary murine hematopoietic progenitor cells that HU treatment enhances AAV-mediated transduction by increasing the trafficking of the virus into the nucleus (M. Tan, K. Qing, J. Hansen, and A. Srivastava, submitted for publication). However, the mechanism by which this occurs is unknown. Because altered endocytic processing of AAV in NIH 3T3 cells impaired transduction efficiency, we hypothesized that the increased nuclear trafficking in response to HU treatment might be due to effects on the endocytic pathway. It has previously been established that inhibition of ribonucleotide reductase by HU occurs after 12 h of treatment (50). Thus, any increase in transduction that occurs when cells are pretreated with HU for less than 12 h may be due to effects of HU on the cell other than inhibition of ribonucleotide reductase. To examine this possibility, we performed a time course experiment in which NIH 3T3 cells were pretreated for various times with 10 mM HU or for 2 h with 750 μM tyrphostin 1, washed, and subsequently infected with vCMVp-*lacZ*. β-Galactosidase activity was measured 48 h postinfection. The results are shown in Fig. 5A. As observed previously (18), tyrphostin 1 pretreatment of NIH 3T3 cells led to a modest increase in transduction efficiency compared with mock-treated cells and pretreatment with HU for 24 h resulted in a significant increase in transduction. The HU-induced increase in transduction was seen as early as 2 h after addition of the drug, indicating that mechanisms other than inhibition of ribonucleotide reductase might be responsible for increasing the AAV-mediated transduction in response to HU. We therefore postulated that HU might increase the transduction of NIH 3T3 cells by altering endocytic processing of AAV, causing virions to pass through dense acidic vesicles prior to nuclear translocation. To test this hypothesis, we infected mock- or HU-treated NIH 3T3 cells with vCMVp-*lacZ* for 1 h at 37°C, fractionated the cellular mem-

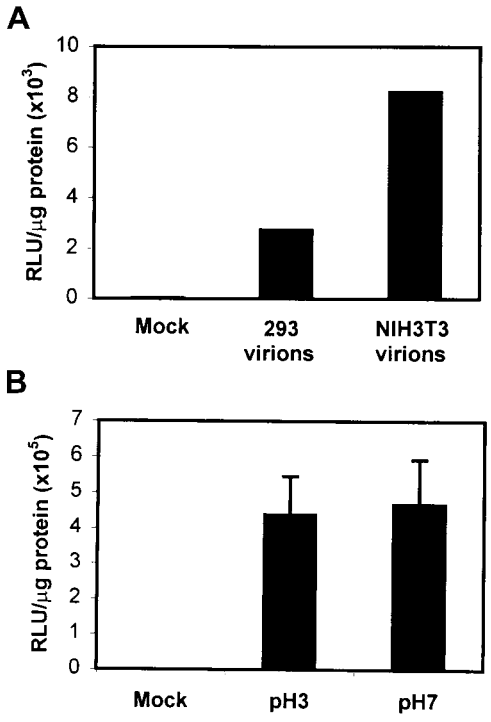

FIG. 4. (A) Infectivity of AAV isolated from the cytoplasm of cells. Virions were isolated from the cytoplasm of vCMVp-luc-infected 293 (293 virions) or NIH 3T3 (NIH 3T3 virions) cells as described in Materials and Methods. After the physical particle titer of the isolated virions was determined by slot blot analysis, 293 cells were either mock infected or infected with equivalent numbers of AAV particles and the luciferase activity was measured 48 h later. Values are expressed in RLU per microgram of total protein. These results are representative of data from two independent experiments. (B) Effect of pH on the transducing ability of AAV. vCMVp-luc was incubated for 30 min at 37°C in buffers of pH 3.0 or 7.0, diluted 100-fold in IMDM, and then used to infect 293 cells (5,000 particles/cell). Luciferase activity was measured 48 h postinfection as described for panel A.

branes as described above, and then detected viral DNA in each fraction by slot blot analysis. These results are shown in Fig. 5B. As expected, little viral DNA was present in the denser vesicles of mock-treated cells. However, in cells treated with HU, the viral DNA could be readily detected in both light and dense fractions, indicating that HU indeed caused the cells to route the incoming virions through dense vesicles. Figure 5C represents the average quantity of viral DNA in each fraction from three independent experiments. Since AAV was processed in dense, acidic vesicles in HU-treated NIH 3T3 cells, we reasoned that Baf treatment might abrogate the HU-mediated increase in transduction. We therefore performed transduction assays in which HU-treated NIH 3T3 cells were either mock treated or treated with 20 nM Baf. These results are shown in Fig. 5D. In contrast to the transduction data for NIH 3T3 cells depicted in Fig. 3A, we noted that Baf caused a significant decrease in transduction efficiency of HU-treated NIH 3T3 cells. This inhibitory effect of Baf on the transduction of HU-treated NIH 3T3 cells was similar to that noted previously in untreated 293 cells (Fig. 3A). Together, these results provided strong evidence that HU treatment of the less permissive NIH 3T3 cells redirects viral processing through dense, acidic endosomes similar to the trafficking patterns observed in highly permissive 293 cells.

DISCUSSION

It has become increasingly clear that multiple obstacles to high-efficiency AAV-mediated transduction of certain cell types exist. We and others have previously shown that the lack of the viral receptors and coreceptors in particular cell types prevents binding and internalization of the virus (35, 39, 48, 49). Transfection of these cells with cDNAs encoding the viral receptors and coreceptors renders them susceptible to transduction by AAV (39). In addition, we have previously described a model in which a cellular protein, the ssD-BP, binds to the D-sequence at the 3′ end of the viral genome and, when tyrosine phosphorylated, can inhibit viral second-strand DNA synthesis and hence transgene expression (38, 40). By treating cells with inhibitors of tyrosine kinases such as genestein or tyrphostin 1, we have demonstrated that the ssD-BP becomes dephosphorylated and therefore allows for efficient viral second-strand DNA synthesis and AAV-mediated transduction (26). Recently, we also identified obstacles in the intracellular trafficking of AAV from the plasma membrane to the nucleus in certain cell types (18). In addition, Duan et al. have reported that ubiquitination of capsid proteins in an apical airway epithelial cell system causes proteasome-mediated degradation of incoming capsids with a concomitant decrease in the transduction efficiency of this cell type (10). Upon treatment of apical airway epithelial cells with a proteasome inhibitor, the AAV transduction efficiency increased in these cells. More recently, we observed that impaired intracellular trafficking into the nuclei of primary murine hematopoietic progenitor cells also contributes, in part, to the low transduction efficiency observed in these cells (Tan et al., submitted).

In the present studies, a systematic analysis of the steps immediately following internalization of the virus into NIH 3T3 and 293 cells has led to the identification of dense endocytic vesicles as a necessary organelle through which AAV must pass prior to efficient translocation to the nucleus. Moreover, processes in these dense endosomes and lysosomes that are dependent on an acidic pH alter the virion and are required for the efficient transduction of permissive cell types. In the less permissive NIH 3T3 cells, the virions fail to traffic through this compartment. Our search to overcome the apparent obstacle of endocytic processing in NIH 3T3 cells led us to the conclusion that HU treatment induces a type of endocytic processing of AAV similar to that observed in 293 cells, with an associated increase in transduction efficiency. Interestingly, this effect is maximal as early as 2 h after the addition of HU, indicating a mechanism other than inhibition of ribonucleotide reductase by HU, which requires about 12 h of treatment.

Based on our current understanding of viral trafficking in 293 and NIH 3T3 cells, we propose a model (Fig. 6). In the permissive 293 cells (Fig. 6A), the virus binds to and enters the cell via clathrin-coated vesicles that mature into early endosomes of relatively low density and neutral pH. Through processes not completely understood, the virions then traffic to late endosomes and/or lysosomes of relatively high density and low pH. Presumably, it is within these dense vesicles that the virion is exposed to some type of modification that is depen-

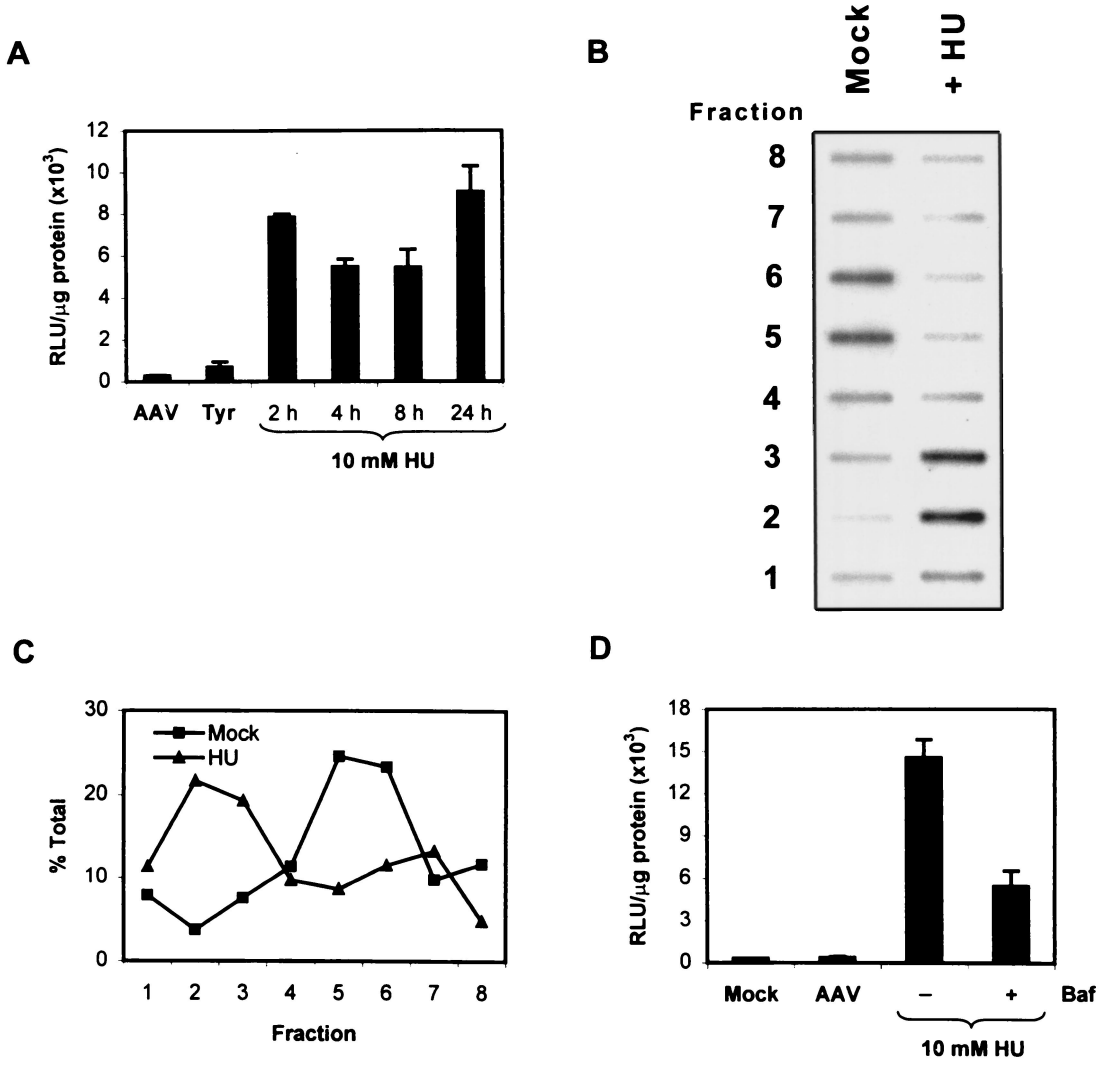

FIG. 5. (A) Time course of transduction of HU-treated NIH 3T3 cells. Cells were either mock treated (AAV), pretreated for various times with 10 mM HU or for 2 h with 750 μM Tyrphostin 1 (Tyr), and subsequently infected with vCMVp-*lacZ* (5,000 particles/cell) for 2 h. β-Galactosidase activity was measured 48 postinfection and is expressed as RLU per microgram of protein. (B) Detection of AAV in density-fractionated membranes from HU-treated NIH 3T3 cells. Cells were either mock treated or pretreated with 10 mM HU for 18 h and infected with vCMVp-*lacZ* for 1 h, and endocytic organelles were fractionated on a Percoll density gradient as described in the legend to Fig. 2. Viral DNA in each fraction was detected by slot blot analysis as described in the legend to Fig. 1. (C) Localization of AAV in subcellular fractions. Autoradiograms similar to that in panel B from three separate experiments were densitometrically scanned, and the signal in each fraction was quantified, averaged, and plotted as a percentage of the total signal. (D) Effect of Baf on AAV-mediated transduction of HU-treated NIH 3T3 cells. The cells were either mock treated (AAV) or treated with 10 mM HU for 18 h. Following a 1-h incubation in medium with or without 20 nM Baf, the cells were mock infected or infected with vCMVp-*lacZ* (5,000 particles/cell) for 2 h, and β-galactosidase activity was measured 48 h postinfection. Data are expressed as RLU per microgram of protein.

dent on low pH and that results in increased trafficking of the virus into the nucleus. Therefore, treatment of cells with compounds that block endosomal acidification will also block trafficking of the virus into the nucleus and transduction. Because treatment of 293 cells with Baf efficiently inhibits the trafficking of AAV into the nucleus, we presume that most of the virions that enter the nucleus have passed through the dense, acidic endosomes. However, although we cannot rule out the possibility that some of the virions in the nucleus escape from early endosomes, this most probably is not a major pathway. In fact, in untreated NIH 3T3 cells (Fig. 6B), most of the virions are processed solely in the early endosomes prior to their escape into the cytoplasm, yet these virions are able to traffic into the nucleus, albeit to a very limited extent. However, treatment of NIH 3T3 cells with HU allows AAV to pass into the dense, acidic vesicles similar to the trafficking observed in 293 cells. While the mechanism responsible for this effect remains to be elucidated, it is interesting that others have demonstrated an increase in the stability of lysosomes prepared from HU-treated murine lymphoblasts compared to the stability of those prepared from untreated cells (37). It is conceivable, therefore, that HU treatment of NIH 3T3 cells may also stabilize the

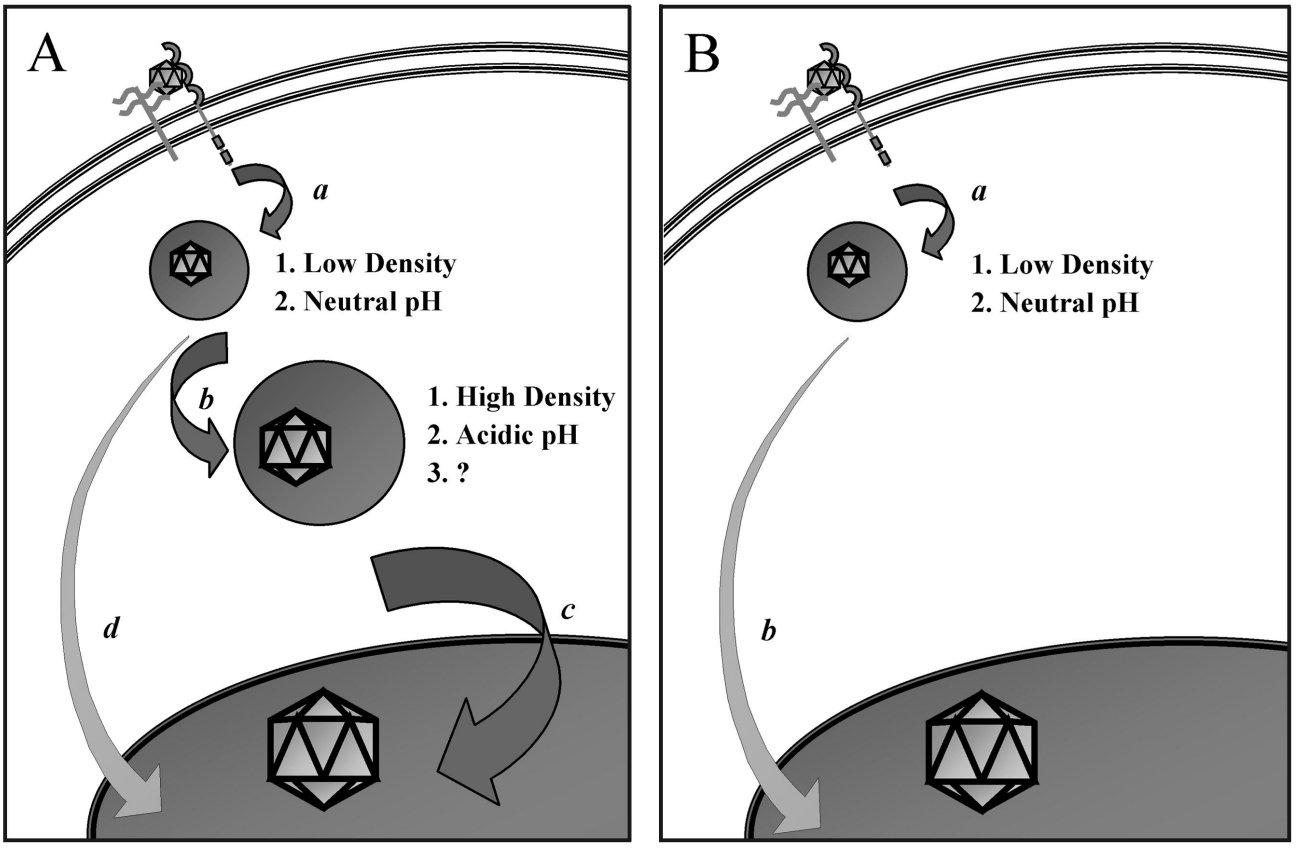

FIG. 6. Hypothetical model comparing intracellular trafficking of AAV in 293 (A) and NIH 3T3 (B) cells. AAV binds and enters the early endosomes of both cell types efficiently (*a*). In 293 cells, most of the virions progress down the endocytic pathway (*b*), enter a dense endocytic organelle with a low pH, undergo a putative capsid modification (?), and subsequently enter the nucleus by an unknown mechanism (*c*). This process can be blocked by inhibitors of endosomal acidification, in which case virions enter the nucleus by a less efficient pathway (*d*). In contrast to the viral trafficking observed in 293 cells, the virions in NIH 3T3 cells fail to pass through dense, acidic endosomes and therefore do not traffic efficiently to the nucleus. Instead, AAV escapes from early endosomes and inefficiently enters the nucleus by an alternate route (*b*).

dense endocytic organelles or lysosomes, increasing the likelihood that the virions will be able to traffic through these compartments. Whether this effect is common to murine cell lines in general remains to be established.

While HU treatment of NIH 3T3 cells induces a pattern of AAV trafficking that is generally similar to that observed in 293 cells, there is a noticeable difference. As shown in Fig. 2C, the virions isolated from infected 293 cells localize to the dense vesicles found in the first, most dense fraction of the density gradient. However, in HU-treated NIH 3T3 cells, while there are more AAV particles in the first fraction than in mock-treated cells, the majority are found in the second fraction of the density gradient (Fig. 5C). These findings would indicate that HU treatment of NIH 3T3 cells shifts the trafficking of AAV to a dense endocytic compartment, but perhaps to a different population of dense endosomes from that observed in 293 cells. Since acid β-galactosidase activity, a classical marker for lysosomes, is located predominantly in the first fraction and to a lesser extent in the second fraction, the virions in 293 cells could traffic to the lysosomes whereas those in HU-treated NIH 3T3 cells might pass through a less dense endocytic compartment such as late endosomes. Separation of membranes on higher-resolution density gradients and a more thorough analysis of endocytic markers in fractions of this gradient are necessary to resolve this issue. However, regardless of whether the virions enter the dense vesicles in fraction 1 or fraction 2, it is clear that the transduction efficiency increases.

Various signaling pathways have been implicated in the control of endocytosis and vesicular transport. For instance, certain members of the PI3-kinase family are known to play a regulatory role in protein trafficking and sorting within the endocytic pathway (28, 30). In fact, mutations in the PI3-kinase family member Fab1p are known to block the transport of integral plasma membrane glycoproteins from endosomes to lysosomes (31). Since others have demonstrated a role for PI3-kinase in AAV-mediated transduction of HeLa cells (45), it is plausible that attenuation of PI3-kinase activity in the less permissive NIH 3T3 cells could account for the decreased transport of AAV from early endosomes to late endosomes and lysosomes and that HU treatment could alter the cellular environment such that PI3-kinase activity, and hence viral trafficking down the endocytic pathway, increases. However, the relative PI3-kinase activity in mock- and HU-treated NIH 3T3 cells remains to be determined. It is interesting that Sanlioglu et al. have demonstrated AAV-mediated activation of PI3-kinase within the first 5 min of infection in HeLa cells (45).

Furthermore, treatment of cells with wortmannin, an inhibitor of PI3-kinase, inhibited the trafficking of AAV into the nucleus. Given the rapid onset, perhaps binding of AAV to a cellular receptor is sufficient to activate PI3-kinase, resulting in trafficking of the virus down the endocytic pathway into dense vesicles. A more thorough investigation of the cellular receptors on NIH 3T3 cells that are involved in viral binding, as well as studies of the PI3-kinase status in these cells, is warranted.

Although events involved in the cytoplasmic processing of AAV in various cell types are becoming increasingly clear, little is known about translocation of the virus from the cytoplasm into the nucleus. Based on preliminary evidence from other laboratories, it has been suggested that intact AAV enters the nucleus where, it is uncoated to release the single-stranded viral genome followed by second-strand DNA synthesis (6, 45). However, direct evidence that intact AAV enters the nucleus is lacking. We have examined this possibility by infecting purified nuclei with AAV in vitro and have demonstrated that AAV can indeed enter isolated nuclei and undergo uncoating and viral second-strand DNA synthesis (J. Hansen, K. Qing, and A. Srivastava, submitted for publication).

Based on the data presented here, it appears that prior to nuclear entry, the capsid structure of AAV isolated from the cytoplasm of 293 cells undergoes some type of modification compared with that of AAV isolated from the cytoplasm of NIH3T3 cells (Fig. 3A). The exact nature of this structural change is currently undefined, but it probably occurs within dense endosomes and may be required for efficient trafficking of the virion into the nucleus. This scenario is reminiscent of the process by which adenovirus, a helper virus for AAV, undergoes putative capsid changes during intracellular transport through acidic vesicles, which are essential for the translocation of the viral genome into the nucleus (17, 32). While it is known that exposure to low pH alone is sufficient for the structural change observed in the adenovirus capsid, our data indicate that in AAV, exposure to low pH is necessary but not sufficient (Fig. 4). Since the virion would encounter many enzymes within the endocytic vesicles, some of which are active only in an acidic environment, it is not surprising that the AAV capsid change may be dependent on one or more of these enzymatic activities. For instance, proteolytic cleavage or reduction of certain residues of the AAV capsid may alter subsequent trafficking events. Studies to determine the function of the AAV capsid changes that occur during endocytic processing on nuclear import, as well as the mechanism by which AAV is transported into the nucleus, would yield crucial information on how cells may further regulate AAV-mediated transduction.

In sum, our studies have identified crucial endocytic processing events involved in AAV-mediated transduction. Moreover, we have shown that HU treatment of cells deficient in these steps restores the processing mechanisms that lead to increased nuclear trafficking and hence to AAV-mediated transduction in less permissive cell types. Further studies of the mechanisms of intracellular processing and transport across the nuclear envelope in permissive and less-permissive cell types will lay the foundation for the development of additional strategies that might surmount these barriers to high-efficiency AAV-mediated transduction and ultimately improve the utility of AAV as vectors for human gene therapy.

ACKNOWLEDGMENTS

We thank John Lich and Janice S. Blum for helpful advice on subcellular fractionation techniques.

This research was supported in part by Public Health Service grant HL-58881 from the National Institutes of Health and a grant from the Phi Beta Psi Sorority.

REFERENCES

1. **Alexander, I. E., D. W. Russell, and A. D. Miller.** 1994. DNA-damaging agents greatly increase the transduction of nondividing cells by adeno-associated virus vectors. J. Virol. **68:**8282–8287.
2. **Alexander, I. E., D. W. Russell, A. M. Spence, and A. D. Miller.** 1996. Effects of gamma irradiation on the transduction of dividing and nondividing cells in brain and muscle of rats by adeno-associated virus vectors. Hum Gene Ther. **7:**841–850.
3. **Atchison, R. W., B. C. Casto, and W. M. Hammon.** 1965. Adenovirus-associated defective virus particles. Science **149:**754–756.
4. **Bachmann, P. A., M. D. Hoggan, E. Kurstak, J. L. Melnick, H. G. Pereira, P. Tattersall, and C. Vago.** 1979. Parvoviridae: second report. Intervirology **11:**248–254.
5. **Bartlett, J. S., J. Kleinschmidt, R. C. Boucher, and R. J. Samulski.** 1999. Targeted adeno-associated virus vector transduction of nonpermissive cells mediated by a bispecific F(ab′gamma)$_2$ antibody. Nat. Biotechnol. **17:**181–186.
6. **Bartlett, J. S., R. Wilcher, and R. J. Samulski.** 2000. Infectious entry pathway of adeno-associated virus and adeno-associated virus vectors. J. Virol. **74:**2777–2785.
7. **Berns, K. I., and R. A. Bohenzky.** 1987. Adeno-associated viruses: an update. Adv. Virus Res. **32:**243–306.
8. **Berns, K. I., and C. Giraud.** 1996. Biology of adeno-associated virus. Curr. Top. Microbiol. Immunol. **218:**1–23.
9. **Duan, D., Q. Li, A. W. Kao, Y. Yue, J. E. Pessin, and J. F. Engelhardt.** 1999. Dynamin is required for recombinant adeno-associated virus type 2 infection. J. Virol. **73:**10371–10376.
10. **Duan, D., Y. Yue, Z. Yan, J. Yang, and J. F. Engelhardt.** 2000. Endosomal processing limits gene transfer to polarized airway epithelia by adeno-associated virus. J. Clin. Investig. **105:**1573–1587.
11. **Ferrari, F. K., T. Samulski, T. Shenk, and R. J. Samulski.** 1996. Second-strand synthesis is a rate-limiting step for efficient transduction by recombinant adeno-associated virus vectors. J. Virol. **70:**3227–3234.
12. **Fisher, K. J., G. P. Gao, M. D. Weitzman, R. DeMatteo, J. F. Burda, and J. M. Wilson.** 1996. Transduction with recombinant adeno-associated virus for gene therapy is limited by leading-strand synthesis. J. Virol. **70:**520–532.
13. **Flotte, T. R., and B. J. Carter.** 1995. Adeno-associated virus vectors for gene therapy. Gene Ther. **2:**357–362.
14. **Geuze, H. J.** 1998. The role of endosomes and lysosomes in MHC class II functioning. Immunol. Today **19:**282–287.
15. **Gjoen, T., T. O. Berg, and T. Berg.** 1997. Lysosomes and endocytosis, p. 169–203. *In* J. M. Graham and D. Rickwood (ed.), Subcellular fractionation—a practical approach. Oxford University Press, Inc., New York, N.Y.
16. **Goldstein, J. L., M. S. Brown, R. G. W. Anderson, D. W. Russell, and W. J. Schneider.** 1985. Receptor-mediated endocytosis: concepts emerging from the LDL receptor system. Annu. Rev. Cell Biol. **1:**1–39.
17. **Greber, U. F., M. Willetts, P. Webster, and A. Helenius.** 1993. Stepwise dismantling of adenovirus 2 during entry into cells. Cell **75:**477–486.
18. **Hansen, J., K. Qing, H. J. Kwon, C. Mah, and A. Srivastava.** 2000. Impaired intracellular trafficking of adeno-associated virus type 2 vectors limits efficient transduction of murine fibroblasts. J. Virol. **74:**992–996.
19. **Hinton, R. H., and B. M. Mullock.** 1997. Isolation of subcellular fractions, p. 31–69. *In* J. M. Graham and D. Rickwood (ed.), Subcellular fractionation—a practical approach. Oxford University Press, Inc., New York, N.Y.
20. **Jensen, P. E.** 1995. Antigen unfolding and disulfide reduction in antigen presenting cells. Semin. Immunol. **7:**347–353.
21. **Kay, M. A., C. S. Manno, M. V. Ragni, P. J. Larson, L. B. Couto, A. McClelland, B. Glader, A. J. Chew, S. J. Tai, R. W. Herzog, V. Arruda, F. Johnson, C. Scallan, E. Skarsgard, A. W. Flake, and K. A. High.** 2000. Evidence for gene transfer and expression of factor IX in haemophilia B patients treated with an AAV vector. Nat. Genet. **24:**257–261.
22. **Kotin, R. M., J. C. Menninger, D. C. Ward, and K. I. Berns.** 1991. Mapping and direct visualization of a region-specific viral DNA integration site on chromosome 19q13-qter. Genomics **10:**831–834.
23. **Kotin, R. M., M. Siniscalco, R. J. Samulski, X. D. Zhu, L. Hunter, C. A. Laughlin, S. McLaughlin, N. Muzyczka, M. Rocchi, and K. I. Berns.** 1990. Site-specific integration by adeno-associated virus. Proc. Natl. Acad. Sci. USA **87:**2211–2215.
24. **Kube, D. M., S. Ponnazhagan, and A. Srivastava.** 1997. Encapsidation of adeno-associated virus type 2 Rep proteins in wild-type and recombinant progeny virions: Rep-mediated growth inhibition of primary human cells. J. Virol. **71:**7361–7371.
25. **Kube, D. M., and A. Srivastava.** 1997. Quantitative DNA slot blot analysis:

inhibition of DNA binding to membranes by magnesium ions. Nucleic Acids Res. **25:**3375–3376.
26. **Mah, C., K. Qing, B. Khuntirat, S. Ponnazhagan, X.-S. Wang, D. M. Kube, M. C. Yoder, and A. Srivastava.** 1998. Adeno-associated virus type 2-mediated gene transfer: role of epidermal growth factor receptor protein tyrosine kinase in transgene expression. J. Virol. **72:**9835–9843.
27. **Manning, W. C., S. Zhou, M. P. Bland, J. A. Escobedo, and V. Dwarki.** 1998. Transient immunosuppression allows transgene expression following readministration of adeno-associated viral vectors. Hum. Gene Ther. **9:**477–485.
28. **Memmo, L. M., and P. McKeown-Longo.** 1998. The alphavbeta5 integrin functions as an endocytic receptor for vitronectin. J. Cell Sci. **111:**425–433.
29. **Nahreini, P., M. J. Woody, S. Z. Zhou, and A. Srivastava.** 1993. Versatile adeno-associated virus 2-based vectors for constructing recombinant virions. Gene **124:**257–262.
30. **Ng, T., D. Shima, A. Squire, P. I. Bastiaens, S. Gschmeissner, M. J. Humphries, and P. J. Parker.** 1999. PKCα regulates β1 integrin-dependent cell motility through association and control of integrin traffic. EMBO J. **18:**3909–3923.
31. **Odorizzi, G., M. Babst, and S. D. Emr.** 1998. Fab1p PtdIns(3)P 5-kinase function essential for protein sorting in the multivesicular body. Cell **95:**847–858.
32. **Pastan, I., P. Seth, D. Fitzgerald, and M. Willingham.** 1986. Adenovirus entry into cells: some new observations on an old problem. Springer-Verlag, New York, N.Y.
33. **Ponnazhagan, S., P. Mukherjee, X.-S. Wang, K. Qing, D. M. Kube, C. Mah, C. Kurpad, M. C. Yoder, E. F. Srour, and A. Srivastava.** 1997. Adeno-associated virus type 2-mediated transduction in primary human bone marrow-derived $CD34^+$ hematopoietic progenitor cells: donor variation and correlation of transgene expression with cellular differentiation. J. Virol. **71:**8262–8267.
34. **Ponnazhagan, S., P. Mukherjee, M. C. Yoder, X.-S. Wang, S. Z. Zhou, J. Kaplan, S. Wadsworth, and A. Srivastava.** 1997. Adeno-associated virus 2-mediated gene transfer in vivo: organ-tropism and expression of transduced sequences in mice. Gene **190:**203–210.
35. **Ponnazhagan, S., X.-S. Wang, M. J. Woody, F. Luo, L. Y. Kang, M. L. Nallari, N. C. Munshi, S. Z. Zhou, and A. Srivastava.** 1996. Differential expression in human cells from the p6 promoter of human parvovirus B19 following plasmid transfection and recombinant adeno-associated virus 2 (AAV) infection: human megakaryocytic leukaemia cells are nonpermissive for AAV infection. J. Gen. Virol. **77:**1111–1122.
36. **Ponnazhagan, S., M. C. Yoder, and A. Srivastava.** 1997. Adeno-associated virus type 2-mediated transduction of murine hematopoietic cells with long-term repopulating ability and sustained expression of a human globin gene in vivo. J. Virol. **71:**3098–3104.
37. **Przybyszewski, W. M., B. Czartoryska, and J. Malec.** 1985. Effect of hydroxyurea treatment on lysosomal membrane stability and enzyme latency in L5178Y cells in culture. Neoplasma **33:**27–31.
38. **Qing, K., B. Khuntirat, C. Mah, D. M. Kube, X.-S. Wang, S. Ponnazhagan, S. Zhou, V. J. Dwarki, M. C. Yoder, and A. Srivastava.** 1998. Adeno-associated virus type 2-mediated gene transfer: correlation of tyrosine phosphorylation of the cellular single-stranded D sequence-binding protein with transgene expression in human cells in vitro and murine tissues in vivo. J. Virol. **72:**1593–1599.
39. **Qing, K., C. Mah, J. Hansen, S. Zhou, V. Dwarki, and A. Srivastava.** 1999. Human fibroblast growth factor receptor 1 is a co-receptor for infection by adeno-associated virus 2. Nat. Med. **5:**71–77.
40. **Qing, K., X.-S. Wang, D. M. Kube, S. Ponnazhagan, A. Bajpai, and A. Srivastava.** 1997. Role of tyrosine phosphorylation of a cellular protein in adeno-associated virus 2-mediated transgene expression. Proc. Natl. Acad. Sci. USA **94:**10879–10884.
41. **Riese, R. J., P. R. Wolf, D. Bromme, L. R. Natkin, J. A. Villandangos, and H. L. Ploegh.** 1996. Essential role for cathepsin S in MHC class II-associated invariant chain processing and peptide loading. Immunity **4:**357–366.
42. **Russell, D. W., I. E. Alexander, and A. D. Miller.** 1995. DNA synthesis and topoisomerase inhibitors increase transduction by adeno-associated virus vectors. Proc. Natl. Acad. Sci. USA **92:**5719–5723.
43. **Sambrook, J., E. Fritsch, and T. Maniatis.** 1989. Molecular cloning: a laboratory manual, 2nd ed., vol. 3. Cold Spring Harbor Laboratory Press, Cold Spring Harbor, N.Y.
44. **Samulski, R. J., X. Zhu, X. Xiao, J. D. Brook, D. E. Housman, N. Epstein, and L. A. Hunter.** 1991. Targeted integration of adeno-associated virus (AAV) into human chromosome 19. EMBO J. **10:**3941–3950.
45. **Sanlioglu, S., P. K. Benson, J. Yang, E. M. Atkinson, T. Reynolds, and J. F. Engelhardt.** 2000. Endocytosis and nuclear trafficking of adeno-associated virus type 2 are controlled by rac 1 and phosphatidylinositol-3 kinase activation. J. Virol. **74:**9184–9196.
46. **Sopelsa, A. M., M. H. Severini, C. M. Da Silva, P. R. Tobo, R. Giugliani, and J. C. Coelho.** 2000. Characterization of beta-galactosidase in leukocytes and fibroblasts of GM1 gangliosidosis heterozygotes compared to normal subjects. Clin. Biochem. **33:**125–129.
47. **Srivastava, A., E. W. Lusby, and K. I. Berns.** 1983. Nucleotide sequence and organization of the adeno-associated virus 2 genome. J. Virol. **45:**555–564.
48. **Summerford, C., J. S. Bartlett, and R. J. Samulski.** 1999. αVβ5 integrin: a co-receptor for adeno-associated virus type 2 infection. Nat. Med. **5:**78–82.
49. **Summerford, C., and R. J. Samulski.** 1998. Membrane-associated heparan sulfate proteoglycan is a receptor for adeno-associated virus type 2 virions. J. Virol. **72:**1438–1445.
50. **Wadler, S., R. Horowitz, J. Rao, X. Mao, K. Schlesinger, and E. L. Schwartz.** 1996. Interferon augments the cytotoxicity of hydroxyurea without enhancing its activity against the M2 subunit of ribonucleotide reductase: effects in wild-type and resistant human colon cancer cells. Cancer Chemother. Pharmacol. **38:**522–528.
51. **Wang, X.-S., B. Khuntirat, K. Qing, S. Ponnazhagan, D. M. Kube, S. Zhou, V. J. Dwarki, and A. Srivastava.** 1998. Characterization of wild-type adeno-associated virus type 2-like particles generated during recombinant viral vector production and strategies for their elimination. J. Virol. **72:**5472–5480.